

2012

## Competition between the crystal field and the exchange field in Er<sup>3+</sup> doped NdMnO<sub>3</sub>

Fang Hong  
*University of Wollongong, fh640@uowmail.edu.au*

Zhenxiang Cheng  
*University of Wollongong, cheng@uow.edu.au*

Xiaolin Wang  
*University of Wollongong, xiaolin@uow.edu.au*

S X. Dou  
*University of Wollongong, shi@uow.edu.au*

Follow this and additional works at: <https://ro.uow.edu.au/engpapers>

 Part of the [Engineering Commons](#)

<https://ro.uow.edu.au/engpapers/5072>

---

### Recommended Citation

Hong, Fang; Cheng, Zhenxiang; Wang, Xiaolin; and Dou, S X.: Competition between the crystal field and the exchange field in Er<sup>3+</sup> doped NdMnO<sub>3</sub> 2012.  
<https://ro.uow.edu.au/engpapers/5072>

## Competition between the crystal field and the exchange field in Er<sup>3+</sup> doped NdMnO<sub>3</sub>

Fang Hong, Zhenxiang Cheng, Xiaolin Wang, and Shixue Dou

Citation: *Appl. Phys. Lett.* **101**, 121913 (2012); doi: 10.1063/1.4754613

View online: <http://dx.doi.org/10.1063/1.4754613>

View Table of Contents: <http://apl.aip.org/resource/1/APPLAB/v101/i12>

Published by the American Institute of Physics.

---

### Related Articles

Ferromagnetic resonance analysis of internal effective field of classified grains by switching field for granular perpendicular recording media

*J. Appl. Phys.* **111**, 07B722 (2012)

Quantitative interpretation of the very fast electronic relaxation of most Ln<sup>3+</sup> ions in dissolved complexes  
*J. Chem. Phys.* **136**, 074513 (2012)

Magnetism and superconductivity in the Heusler alloy Pd<sub>2</sub>YbPb  
*J. Appl. Phys.* **111**, 07E111 (2012)

Control of the exchange coupling in granular CoPt/Co recording media  
*J. Appl. Phys.* **109**, 07B752 (2011)

First principles study on the local magnetic anisotropy near surfaces of Dy<sub>2</sub>Fe<sub>14</sub>B and Nd<sub>2</sub>Fe<sub>14</sub>B magnets  
*J. Appl. Phys.* **109**, 07A702 (2011)

---

### Additional information on *Appl. Phys. Lett.*

Journal Homepage: <http://apl.aip.org/>

Journal Information: [http://apl.aip.org/about/about\\_the\\_journal](http://apl.aip.org/about/about_the_journal)

Top downloads: [http://apl.aip.org/features/most\\_downloaded](http://apl.aip.org/features/most_downloaded)

Information for Authors: <http://apl.aip.org/authors>

### ADVERTISEMENT

The advertisement features a blue background on the left with the text 'AMERICAN PHYSICAL SOCIETY'S OPEN ACCESS JOURNAL' in white. On the right, there is a graphic with a red and purple gradient background. It includes the large white letters 'PRX' and a stylized white logo of two overlapping circles. To the right of the logo, the text 'Committed to Excellence' is written in white, followed by 'Physical Review X' and the website 'prx.aps.org' in a smaller white font.

## Competition between the crystal field and the exchange field in Er<sup>3+</sup> doped NdMnO<sub>3</sub>

Fang Hong, Zhenxiang Cheng,<sup>a)</sup> Xiaolin Wang, and Shixue Dou

*Institute for Superconducting and Electronic Materials, University of Wollongong, Wollongong, NSW 2519, Australia*

(Received 1 May 2012; accepted 10 September 2012; published online 20 September 2012)

A careful investigation of specific heat shows that the ground state splitting of Nd<sup>3+</sup> has been modified by the Er<sup>3+</sup> doping, as it shows a nonlinear dependence on the Er<sup>3+</sup> doping rate, due to the competition between the crystal field and the exchange field. This competition could be further confirmed by the anomalies in the magnetic entropy and the ground state splitting found in Nd<sub>0.9</sub>Er<sub>0.1</sub>MnO<sub>3</sub>. On the contrary, the ground state splitting of Er<sup>3+</sup> has a linear dependence on the doping rate, indicating its stronger dependence on the crystal field rather than the exchange field.

© 2012 American Institute of Physics. [<http://dx.doi.org/10.1063/1.4754613>]

The perovskite LaMnO<sub>3</sub> is a classic manganite, a good study subject and the object of great physical interest, in which the Jahn-Teller distortion and the orbital ordering play a critical role in determining the antiferromagnetic interaction.<sup>1</sup> It shows typical A-type antiferromagnetism (AFM) at 140 K because of the orbital ordering.<sup>2</sup> When divalent ions are doped into the La<sup>3+</sup> sites, such as La<sub>1-x</sub>Ca<sub>x</sub>MnO<sub>3</sub>,<sup>3</sup> the manganese ions will be in the forms of both Mn<sup>3+</sup> and Mn<sup>4+</sup>, allowing the magnetoresistance effect to occur.<sup>4,5</sup> On the other hand, when the La<sup>3+</sup> site is totally replaced by other rare earth ions, unique physical properties can be observed. A-type AFM still exists in SmMnO<sub>3</sub>, in which Sm<sup>3+</sup> has a smaller ionic radius than that of La<sup>3+</sup>, but it is a canted A-type AFM with a weak ferromagnetic (FM) component.<sup>6</sup> The complex magnetic phase diagram and multiferroic properties have been well studied in DyMnO<sub>3</sub> and TbMnO<sub>3</sub>.<sup>7,8</sup> When La<sup>3+</sup> is replaced by much smaller atoms, such as Er<sup>3+</sup>, extremely strong distortion will be introduced, which favours the hexagonal structure, so that ErMnO<sub>3</sub> has a frustrated triangular spin arrangement on the Mn<sup>3+</sup> sublattice.<sup>9,10</sup> It seems that the magnetic rare earth ions do not affect the antiferromagnetic interaction of the Mn<sup>3+</sup> sublattice too much beyond the distortion effect. On the contrary, the low temperature behaviour of magnetic rare earth ions is to some extent modified by the Mn<sup>3+</sup> ordering. When Gd<sup>3+</sup> with 4f electrons is introduced to replace La<sup>3+</sup> in LaMnO<sub>3</sub>,<sup>11</sup> the spin canting of Mn<sup>3+</sup> can polarize the 4f spins in Gd<sup>3+</sup>. A similar result is also reported in SmMnO<sub>3</sub>.<sup>12</sup> It is found that the canted A-type antiferromagnetic ordering of Mn<sup>3+</sup> has a strong effect on Sm<sup>3+</sup> and induces a specific heat anomaly at low temperature, due to splitting of Sm<sup>3+</sup> ground state doublets in the exchange field, crystal field, and external magnetic field.<sup>12</sup> Systematic study of single crystal PrMnO<sub>3</sub> and NdMnO<sub>3</sub> has also indicated that the isotropic and anisotropic exchange fields play a critical role in determining the splitting of rare earth ground states. The Pr<sup>3+</sup> ground state splitting is dominated by the crystal field due to the absence of a ferromagnetic component, while the Nd<sup>3+</sup> ground state splitting is dominated by the exchange field.<sup>13</sup>

Therefore, the low temperature behaviour of magnetic rare earth ions is strongly dependent on the exchange field. At the same time, the exchange field and the crystal field may compete or cooperate with each other. To elucidate this complex behaviour, we studied the specific heat in the Nd<sub>1-x</sub>Er<sub>x</sub>MnO<sub>3</sub> system. Considering that the Er<sup>3+</sup> ion size is a little smaller than that of Nd<sup>3+</sup>, the crystal field could be modified slightly by Er<sup>3+</sup> doping. In addition, our previous work<sup>14</sup> shows that the interaction between Nd<sup>3+</sup> and Mn<sup>3+</sup> is significantly disturbed by Er<sup>3+</sup> doping, and the canted angle of Mn<sup>3+</sup> antiferromagnetic ordering is also consequently modified, which indicates variation in the exchange field. In this case, this is an ideal system to study the relationship between the crystal field and the exchange field. The specific heat study in this system will help to understand the low temperature behaviour of magnetic rare earth ions in other similar systems.

Polycrystalline samples of Nd<sub>1-x</sub>Er<sub>x</sub>MnO<sub>3</sub> (x = 0, 0.1, 0.2, 0.33, 0.5) were made by the traditional solid state reaction method with Nd<sub>2</sub>O<sub>3</sub> (99.9%), Er<sub>2</sub>O<sub>3</sub> (99.9%), and MnCO<sub>3</sub> (99.9%) powder bought from Sigma-Aldrich. Stoichiometric amounts of raw oxide powder were weighed carefully and mixed in an agate mortar, followed by pressing into pellets 15 mm in diameter at 20 MPa. Samples were calcined at 950 °C for 10 h and sintered at 1450 °C for 48 h. The specific heat was measured using the thermal relaxation technique with a 14 T physical properties measurement system (PPMS).

Specific heat measurements were conducted from 2 K to certain temperatures above the magnetic transition temperature. The temperature dependence of Cp/T for samples with x ≤ 0.5 is presented in Figure 1. The peak at higher temperature is assigned to the AFM ordering of Mn<sup>3+</sup>. To calculate the magnetic contribution to the antiferromagnetic transition, a third order polynomial background is subtracted from the experimental data to exclude the contribution from phonons and electrons. A fitting example is presented in Figure 2(a) for the sample with x = 0, and the residual magnetic contributions of all samples are shown in Figure 2(b). It is obvious that the specific heat peaks shift to lower temperature when x increases, which is the result of an enhanced Jahn-Teller effect.<sup>15</sup> The magnetic entropy of magnetic ordering is shown in Figure 2(c), calculated in the form of

<sup>a)</sup>Author to whom correspondence should be addressed. Electronic mail: [cheng@uow.edu.au](mailto:cheng@uow.edu.au).

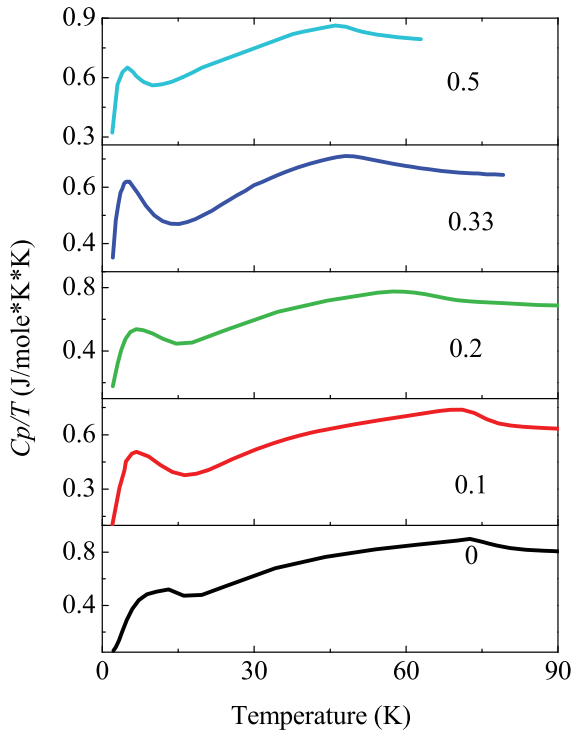


FIG. 1. Temperature dependence of  $C_p/T$  for  $\text{Nd}_{1-x}\text{Er}_x\text{MnO}_3$  for  $x=0, 0.1, 0.2, 0.33$ , and  $0.5$ .

$$S_{\text{Mag}} = \int_{T_1}^{T_2} \left( \frac{\Delta C_p}{T} \right) dT. \quad (1)$$

The magnetic entropy decreases slightly when  $x$  varies from 0 to 0.2 to 0.33. The sample with  $x=0.1$  has the biggest magnetic entropy compared with the others, which is in accordance with the significantly different bond length and bond angle in the sample with  $x=0.1$ .<sup>14</sup> The sample with  $x=0.5$  shows the smallest magnetic entropy, suggesting the weak magnetic contribution.

Below 25 K, there is another  $\lambda$ -shaped peak ascribed to the Schottky anomaly from the ground state doublet splitting of  $\text{Nd}^{3+}$  and/or  $\text{Er}^{3+}$ . For  $\text{NdMnO}_3$ , the long range ordering temperature of  $\text{Nd}^{3+}$  is around 13 K according to the reported result,<sup>14,16</sup> which seems to contribute to the specific heat. However, short range ordering of  $\text{Nd}^{3+}$  is also found to exist above 13 K due to the strong  $\text{Nd}^{3+}\text{-Mn}^{3+}$  interaction,<sup>14,17</sup> similar to the case of  $\text{SmMnO}_3$ .<sup>12</sup> In  $\text{NdNiO}_3$  (Ref. 18) and  $\text{SmMnO}_3$ ,<sup>12</sup> the low temperature shoulders of the specific heat are both supposed to be related to the Schottky anomaly. According to the specific heat study on  $\text{Nd}_{0.67}\text{Sr}_{0.33}\text{MnO}_3$ , the entropy from the Schottky anomaly is only  $\sim 85\%$  of the expected entropy of normal  $\text{Nd}^{3+}$  ordering, suggesting an effective molecular-field mechanism because of the much stronger  $\text{Nd}^{3+}\text{-Mn}^{3+}$  interaction compared to the  $\text{Nd}^{3+}\text{-Nd}^{3+}$  interaction.<sup>19</sup> On the other hand, in  $\text{ErMnO}_3$  and  $\text{YMnO}_3$ , the small shoulder peaks at low temperature are also only attributed to the intrinsic  $\text{Mn}^{3+}$  ordering, but they are modified by the interaction between  $\text{Er}^{3+}/\text{Y}^{3+}$  and  $\text{Mn}^{3+}$  to some extent.<sup>20</sup> Hence, it is reasonable to assign the peaks of specific heat at low temperature mainly to the Schottky anomaly in  $\text{Nd}_{1-x}\text{Er}_x\text{MnO}_3$ . At the same time,

there is also a magnetic contribution from  $\text{Mn}^{3+}$  ordering. To clarify the contribution from the Schottky anomaly and magnetic ordering, specific heat fitting was carried out. Generally, the total specific heat is made up of four distinct contributions: lattice, electron, hyperfine, and magnetic ordering, which can be described as below:

$$C = C_{\text{lat}} + C_{\text{elec}} + C_{\text{hyp}} + C_{\text{mag}}. \quad (2)$$

The lattice contribution can be written as  $C_{\text{lat}} = \beta_3 T^3 + \beta_5 T^5$ . In most cases, the contribution of  $\beta_5 T^5$  is not considered, as it is too small. For a typical antiferromagnetic insulating material, the conductive electron contribution,  $C_{\text{elec}} = \gamma T$ , can be ignored.<sup>12</sup> Likewise, the hyperfine contribution,  $C_{\text{hyp}} = \alpha/T^2$ , is very small above 2 K and can also be ignored.<sup>19</sup>  $\text{LaMnO}_3$  is known as a typical A-type antiferromagnet, and the spin wave excitations could lead to an extra contribution to specific heat and give a  $T^2$  term.<sup>21</sup> The contribution can also be understood to originate from the ferromagnetic and antiferromagnetic spin fluctuations.<sup>22</sup> According to the report of Woodfield *et al.*, an A-type antiferromagnetic spin wave excitation will contribute to specific heat in the form of  $C_{\text{mag}} = 0.058 k_B^3 T^2 / DpDz$ , where  $DpDz$  is the spin wave stiffness coefficient.<sup>21</sup> In our study, this  $T^2$  term contribution should be considered because  $\text{Nd}_{1-x}\text{Er}_x\text{MnO}_3$  is also an A-type antiferromagnetic system. Therefore, the specific heat can be written in a simple way

$$C = C_{\text{lat}} + C_{\text{mag}}. \quad (3)$$

Considering the Schottky anomaly at low temperature, the final specific heat should be in the form of

$$C = C_{\text{lat}} + C_{\text{mag}} + C_{\text{Sch}}, \quad (4)$$

The Schottky anomaly comes from the ground state splitting of the rare earth ions  $\text{Nd}^{3+}$  and/or  $\text{Er}^{3+}$ , and the corresponding specific heat contribution follows the expression:

$$C_{\text{Sch}} = R^* (E/k_B T)^{2*} \exp(E/k_B T) / [1 + \exp(E/k_B T)]^2, \quad (5)$$

where  $R$  is the ideal gas constant,  $E$  is the splitting energy of ground state doublets, and  $k_B$  is the Boltzmann constant.

Figure 3 presents the fitting results of representative samples with  $x=0$  and  $0.2$ . The fitting results of other three samples are given in the supplementary material.<sup>23</sup> The fitting curves well match the experimental data, which is indicative of good fitting quality. It is found that the lattice and spin wave dominate the contributions to the specific heat at relatively higher temperatures. However, the Schottky anomaly plays a more important role at low temperature, especially below 15 K. The  $\text{Nd}^{3+}$  ground state splitting of the sample with  $x=0$  is found to be  $27.8 k_B$ , which is close to the  $\text{Nd}^{3+}$  ground state splitting energy of  $27.15 k_B$  in powder  $\text{NdCrO}_3$ .<sup>24</sup> However, this splitting is bigger than that found in single crystal  $\text{NdMnO}_3$ , in which the splitting is about  $20 k_B$ .<sup>13,25</sup> The difference is probably due to the size effect, which has also been observed in  $\text{Yb}_2\text{Ti}_2\text{O}_7$  (Ref. 26) and  $\text{Gd}^{3+}$  doped  $\text{SrCl}_2$ ,<sup>27</sup> and can affect the crystal field. The splitting of the  $\text{Nd}^{3+}$  ground state doublets decreases to

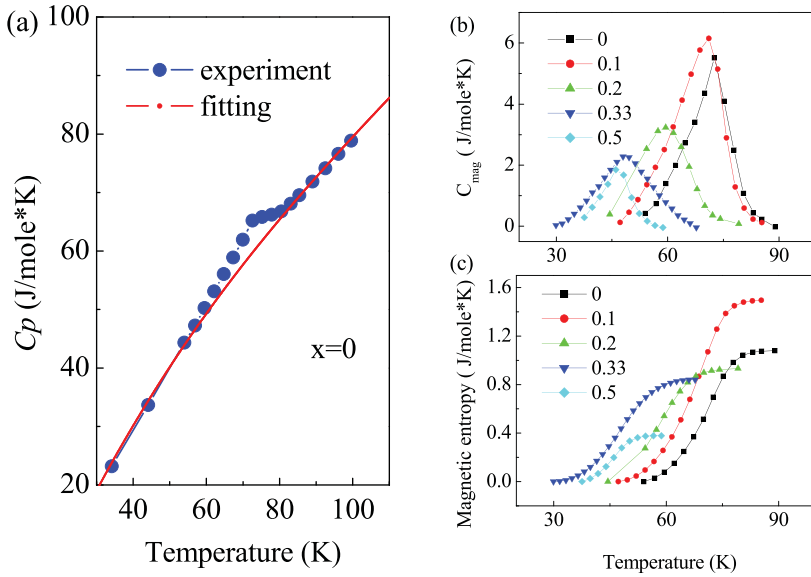


FIG. 2. (a) Phonon and electron contribution to specific heat (small red dotted line) is subtracted from experimental data (big blue dotted line) for the sample with  $x=0$ ; (b) temperature dependence of the residual magnetic contributions to the antiferromagnetic transitions for all samples; (c) temperature dependence of integrated magnetic entropy for all samples calculated from (b).

23.25  $k_B$  when  $x$  is 0.2, and to 26.1  $k_B$  when  $x$  is 0.5. The doping rate dependence of the  $\text{Nd}^{3+}$  ground state splitting energy,  $E_1$ , is plotted in Figure 4(a), where it shows nonlinear behaviour. It is clear that the splitting energies are reduced after doping. We tentatively use a parabolic profile to fit the split-

ting energy curve, except for the data point of the sample with  $x=0.1$  in Figure 4(a), and get an empirical formula

$$E_1 = 28 - 44.4*x + 79.8*x^2. \quad (6)$$

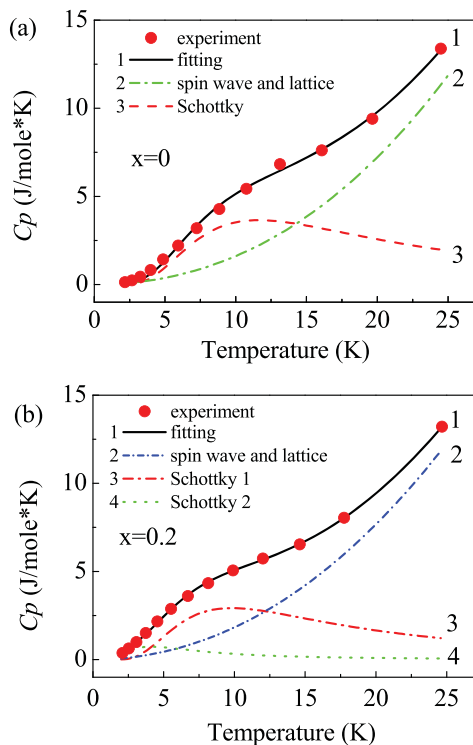


FIG. 3. (a) Low temperature specific heat fitting for sample with  $x=0$  (red dots: experimental data; solid black line: fitting result; green dashed dotted line: spin wave and lattice contribution; red dashed line: Schottky anomaly from ground state splitting of rare earth  $\text{Nd}^{3+}$  ions); (b) low temperature specific heat fitting for sample with  $x=0.2$  (red dots: experimental data; solid black line: fitting result; blue dashed dotted line: spin wave and lattice contribution; red dashed dotted line: Schottky anomaly from ground state splitting of rare earth  $\text{Nd}^{3+}$  ions; green dotted line: Schottky anomaly from ground state splitting of rare earth  $\text{Er}^{3+}$  ions).

After doping with  $\text{Er}^{3+}$ , the static Jahn-Teller distortion becomes stronger, which could induce enhancement of the crystal field, except in the case of  $x=0.1$ . Meanwhile, the interaction between the  $\text{Nd}^{3+}$  and the  $\text{Mn}^{3+}$  ions is significantly disturbed, and the exchange field is consequently reduced. Accordingly, the  $\text{Nd}^{3+}$  ground state splitting energy decreases. This is primarily due to the reduced exchange field, which still plays a dominating role, rather than the enhanced crystal field. As the  $\text{Er}^{3+}$  doping rate  $x$  increases to 0.5, the enhanced crystal field exceeds the exchange field and induces a higher  $\text{Nd}^{3+}$  ground state splitting energy. Therefore, the competition between the exchange field and the crystal field determines the nonlinear doping rate dependence of the  $\text{Nd}^{3+}$  ground state splitting energy. For the sample with  $x=0.1$ , however, the enhanced ferromagnetic component of the  $\text{Mn}^{3+}$  sublattice, corresponding to an enhanced exchange field, fails to induce stronger  $\text{Nd}^{3+}$  ground state doublet splitting. This anomalous splitting possibly stems from the significant lattice change compared with  $x=0.2$  and 0.33,<sup>14</sup> which further confirms the competition between the crystal field and the exchange field.

As for  $\text{Er}^{3+}$ , the ground state doublet splitting energies shown as  $E_2$  in Figure 4(b) are all quite close, around 10  $k_B$ . A tentative linear relation can be found

$$E_2 = 8.5 + 4.5*x. \quad (7)$$

Considering the competition between the exchange field and the crystal field found at the  $\text{Nd}^{3+}$  sites and assuming that a very similar crystal field applies to the  $\text{Er}^{3+}$  sites, this linear behaviour is then mainly dominated by a possible linear change in the crystal field rather than the exchange field. In this case, the interaction between  $\text{Er}^{3+}$  and  $\text{Mn}^{3+}$  should be much weaker compared with that between  $\text{Nd}^{3+}$  and  $\text{Mn}^{3+}$ .

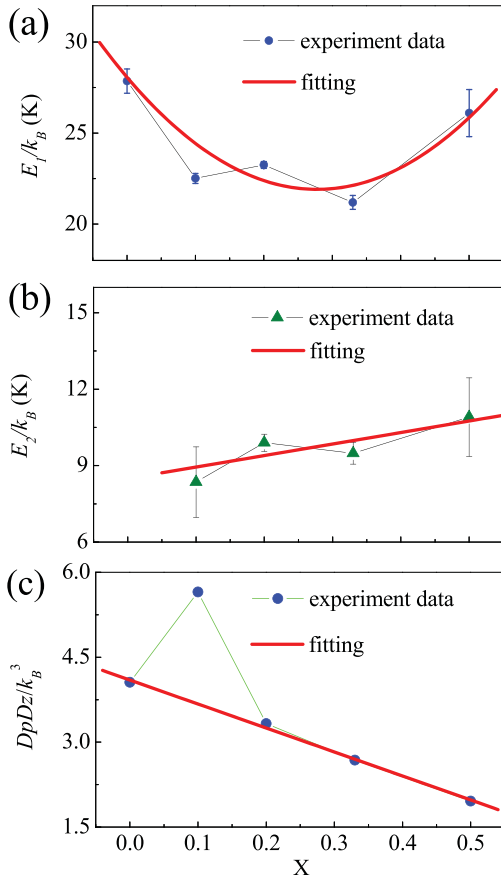


FIG. 4. (a, b) Doping rate dependence of the energy gap between two splitting  $\text{Nd}^{3+}$  ground states ( $E_1$ ) and two splitting  $\text{Er}^{3+}$  ground states ( $E_2$ ). (c) Doping rate dependence of spin wave stiffness coefficient.

On the other hand, if the interaction between  $\text{Er}^{3+}$  and  $\text{Mn}^{3+}$  is comparable to that between  $\text{Nd}^{3+}$  and  $\text{Mn}^{3+}$  or even stronger, then the linear behaviour may suggest that the crystal field should be stronger on  $\text{Er}^{3+}$  than on  $\text{Nd}^{3+}$ . In this case, the crystal field difference suggests that the  $\text{Nd}^{3+}$  and  $\text{Er}^{3+}$  ions could be interacting with each other, considering that only the same crystal field is offered by the  $\text{Mn}^{3+}$  sublattice. Further study is required to elucidate this complex mechanism.

The spin wave stiffness coefficients at low temperature were also obtained and the results are presented in Figure 4(c). Apart from the sample with  $x=0.1$ , the spin wave contributions of the other four samples follow a linear dependence on the doping rate with a negative slope. This behaviour can be fitted by an empirical formula

$$DpDz = (-4.23 \cdot x + 4.10) \cdot k_B^3. \quad (8)$$

The weakening behaviour of the spin wave coefficient with increasing  $\text{Er}^{3+}$  doping is due to the weaker antiferromagnetic interaction of the  $\text{Mn}^{3+}$  sublattice, which is consistent with the decreasing transition temperatures confirmed by the results given in Figures 1 and 2(b). In addition, the weakening behaviour of the spin wave coefficient is also in line with the weaker ground state doublet splitting of  $\text{Nd}^{3+}$ . The anomaly in the spin wave stiffness coefficient for the sample with  $x=0.1$  is probably due to an enhanced ferromagnetic

component induced by the Dzyaloshinsky-Moriya interaction. This anomaly is also the consequent result of the anomaly found in the magnetic entropy at  $x=0.1$  as shown in Figure 2(c).

In summary, the specific heat of the  $\text{Er}^{3+}$  doped rare earth manganate  $\text{NdMnO}_3$  has been systematically studied. There are two clear bumps in the temperature dependence of the specific heat: One is associated with the antiferromagnetic transition of the  $\text{Mn}^{3+}$  sublattice, and the other is due to the Schottky anomaly because of the  $\text{Nd}^{3+}/\text{Er}^{3+}$  ground state doublet splitting. The  $\text{Nd}^{3+}$  ground state splitting energies show a nonlinear dependence on the doping rate. Both the molecular exchange field and the variations in the crystal field are responsible for the ground state doublet splitting, and their competition effect decides the nonlinear behaviour of the doping rate dependent  $\text{Nd}^{3+}$  ground state splitting. The  $\text{Er}^{3+}$  ground state splitting energy is linearly dependent on the doping rate, which is due to the dominance of the crystal field over the exchange field. The spin wave stiffness coefficient can be well fitted by a linear profile with a negative slope, except for the case of  $x=0.1$ . These results provide a quasi-quantitative analysis to determine the relationship between the crystal field and the exchange field, and its effect on magnetic rare earth ions.

Zhenxiang Cheng thanks the Australian Research Council for support through a Future Fellowship (FT 0990287). The authors also thank Dr. Tania Silver for her kind help in revision of the manuscript.

- <sup>1</sup>I. Solovyev, N. Hamada, and K. Terakura, *Phys. Rev. Lett.* **76**, 4825 (1996).
- <sup>2</sup>Y. Murakami, J. P. Hill, D. Gibbs, M. Blume, I. Koyama, M. Tanaka, H. Kawata, T. Arima, Y. Tokura, K. Hirota, and Y. Endoh, *Phys. Rev. Lett.* **81**, 582 (1998).
- <sup>3</sup>A. P. Ramirez, P. Schiffer, S. W. Cheong, C. H. Chen, W. Bao, T. T. M. Palstra, P. L. Gammel, D. J. Bishop, and B. Zegarski, *Phys. Rev. Lett.* **76**, 3188 (1996).
- <sup>4</sup>Y. Moritomo, A. Asamitsu, H. Kuwahara, and Y. Tokura, *Nature* **380**, 141 (1996).
- <sup>5</sup>M. B. Salamon and M. Jaime, *Rev. Mod. Phys.* **73**, 583 (2001).
- <sup>6</sup>J. S. Jung, A. Iyama, H. Nakamura, M. Mizumaki, N. Kawamura, Y. Wakabayashi, and T. Kimura, *Phys. Rev. B* **82**, 212403 (2010).
- <sup>7</sup>T. Kimura, G. Lawes, T. Goto, Y. Tokura, and A. P. Ramirez, *Phys. Rev. B* **71**, 224425 (2005).
- <sup>8</sup>Y. Tokura and S. Seki, *Adv. Mater.* **22**, 1554 (2010).
- <sup>9</sup>M. Fiebig, C. Degenhardt, and R. V. Pisarev, *Phys. Rev. Lett.* **88**, 027203 (2001).
- <sup>10</sup>H. Sugie, N. Iwata, and K. Kohn, *J. Phys. Soc. Jpn.* **71**, 1558 (2002).
- <sup>11</sup>J. Hemberger, S. Lobina, H. A. K. von Nidda, N. Tristan, V. Y. Ivanov, A. A. Mukhin, A. M. Balbashov, and A. Loidl, *Phys. Rev. B* **70**, 024414 (2004).
- <sup>12</sup>J. G. Cheng, J. S. Zhou, J. B. Goodenough, Y. T. Su, Y. Sui, and Y. Ren, *Phys. Rev. B* **84**, 104415 (2011).
- <sup>13</sup>J. Hemberger, M. Brando, R. Wehn, V. Y. Ivanov, A. A. Mukhin, A. M. Balbashov, and A. Loidl, *Phys. Rev. B* **69**, 064418 (2004).
- <sup>14</sup>F. Hong, Z. Cheng, and X. Wang, *Appl. Phys. Lett.* **99**, 192503 (2011).
- <sup>15</sup>T. Kimura, S. Ishihara, H. Shintani, T. Arima, K. T. Takahashi, K. Ishizaka, and Y. Tokura, *Phys. Rev. B* **68**, 060403 (2003).
- <sup>16</sup>A. Munoz, J. A. Alonso, M. J. Martinez-Lopez, J. L. Garcia-Munoz, and M. T. Fernandez-Diaz, *J. Phys.: Condens. Matter* **12**, 1361 (2000).
- <sup>17</sup>S. Jandl, V. Nekvasil, M. Diviš, A. A. Mukhin, J. Hölsä, and M. L. Sadowski, *Phys. Rev. B* **71**, 024417 (2005).
- <sup>18</sup>S. Rosenkranz, M. Medarde, F. Fauth, J. Mesot, M. Zolliker, A. Furrer, U. Staub, P. Lacorre, R. Osborn, R. S. Eccleston, and V. Trounov, *Phys. Rev. B* **60**, 14857 (1999).
- <sup>19</sup>J. E. Gordon, R. A. Fisher, Y. X. Jia, N. E. Phillips, S. F. Reklis, D. A. Wright, and A. Zettl, *Phys. Rev. B* **59**, 127 (1999).

- <sup>20</sup>M. C. Sekhar, S. Lee, G. Choi, C. Lee, and J. G. Park, *Phys. Rev. B* **72**, 014402 (2005).
- <sup>21</sup>B. F. Woodfield, M. L. Wilson, and J. M. Byers, *Phys. Rev. Lett.* **78**, 3201 (1997).
- <sup>22</sup>D. Phelan, D. Louca, S. Rosenkranz, S. H. Lee, Y. Qiu, P. J. Chupas, R. Osborn, H. Zheng, J. F. Mitchell, J. R. D. Copley, J. L. Sarrao, and Y. Moritomo, *Phys. Rev. Lett.* **96**, 027201 (2006).
- <sup>23</sup>See supplementary material at <http://dx.doi.org/10.1063/1.4754613> for other fitting results.
- <sup>24</sup>F. Bartolomé, J. Bartolomé, M. Castro, and J. J. Melero, *Phys. Rev. B* **62**, 1058 (2000).
- <sup>25</sup>J. G. Cheng, Y. Sui, Z. N. Qian, Z. G. Liu, J. P. Miao, X. Q. Huang, Z. Lu, Y. Li, X. J. Wang, and W. H. Su, *Solid State Commun.* **134**, 381 (2005).
- <sup>26</sup>A. Yaouanc, P. Dalmas de Réotier, C. Marin, and V. Glazkov, *Phys. Rev. B* **84**, 172408 (2011).
- <sup>27</sup>M. Rappaz, C. Solliard, A. Châtelain, and L. A. Boatner, *Phys. Rev. B* **21**, 906 (1980).